Anomalous Dynamics in 2D Polymer Melts

H. Meyer and A. N. Semenov

Institut Charles Sadron, CNRS UPR 22, Université de Strasbourg, 23 rue du Loess, 67034 Strasbourg, France

(Received 26 June 2012; published 14 December 2012)

The dynamics in polymer monolayers where chains are strongly confined and adopt 2D conformations are drastically different to those in the bulk. It is shown that viscoelastic hydrodynamic interactions play a major role defining the anomalous chain diffusion properties in such systems where chains cannot cross each other. We developed a quantitative analytical theory of polymer subdiffusion in 2D systems revealing a complex behavior controlled by a delicate interplay of inertial, viscoelastic hydrodynamic interactions, finite-box-size and frictional effects. The theory is fully supported by extensive momentum-conserving and Langevin molecular-dynamics simulation data explaining the highly cooperative character of 2D polymer motions.

DOI: 10.1103/PhysRevLett.109.248304 PACS numbers: 47.57.Ng, 66.20.Cy, 83.80.Sg

Introduction.—It is well-known that classical two-dimensional (2D) fluids show anomalous dynamics (log-diverging viscosity and diffusion coefficients) related to the long-time tail of the velocity autocorrelation function (VAF) of a tagged particle [1–5]. The dynamics of linear polymers confined in 2D monolayers (2D polymer fluids) are even more complex and are not yet well understood, although they have attracted a lot of interest [6–14]. Part of the difficulty is related to nontrivial polymer conformational statistics and dynamics: The chains in such systems stay highly compact and segregated showing fractal (non-Gaussian) conformational properties even at high densities [6–8,15–18]. The chains also show non-Rousean internal dynamics by highly correlated amoebalike motions not involving activation barriers [9,16,19,20].

In view of various nontrivial effects, the challenge to account theoretically for 2D polymer melt dynamics seems to be a formidable problem. We demonstrate here that it is tractable by presenting a quantitative theory of anomalous 2D chain self-diffusion supported by extensive simulation data of a flexible bead-spring model [21], both for momentum-conserving and Langevin molecular dynamics. In both cases we elucidate several regimes of anomalous slow decay in the autocorrelation function of the center-of-mass (c.m.) velocity of a tagged chain.

The most recent attempt to describe the chain diffusion in strictly 2D melts [9] reported molecular dynamics simulations with a standard (moderate) Langevin friction, showing that the motion in 2D melts is highly correlated leading to anomalous diffusion and relaxation of subchains faster than expected for Rouse dynamics. These results were rationalized by scaling arguments. The quantitative approach developed in this Letter is valid for a much larger parameter range and reveals that the scaling approach actually did not consider the main physical mechanism responsible for the anomalous chain diffusion. Ref. [9] assumed that the Langevin friction destroys any hydrodynamic effects. However, we have discovered recently that viscoelastic hydrodynamic interactions (VHI) are important in 3D polymer melts, even with Langevin friction [22,23]. It turns out that they are even more important in 2D. In addition, finite box-size effects need to be included to correctly describe simulations (3D or 2D [5,24]). Although the importance of hydrodynamic and finite size effects has already been recognized for confined or adsorbed polymer dynamics, they were so far only discussed for single chain or dilute systems [24–28].

Overview.—Each chain in a 2D melt occupies a compact region of area $A \simeq N/c_0$ (N is the number of units per chain, c_0 is concentration of these units) and typical size $R = \sqrt{A} = b\sqrt{N}$ ($b = 1/\sqrt{c_0}$ is the monomer size). The area is limited by a fractal boundary whose length $\mathcal{L} \sim b(R/b)^{5/4} \sim bN^{5/8}$ is much longer than R (the fractal dimension of the perimeter is 5/4) [15]. The most important dynamical parameter of the system is the terminal chain conformational relaxation time t_m. The self-similar chain structure and its amoebalike dynamics point to the scaling law $t_m \simeq \tau_1 N^\alpha$ (τ_1 is the monomer time), and it was argued that $\alpha = 3 \cdot 5/8 = 15/8$ [9,16]. The argument is based on the estimate of the maximum energy dissipation at the perimeter line; hence, the value 15/8 should be considered as an upper bound for α. It involves the assumption that a segment located initially at the perimeter line has to follow it during the time $\sim t_m$, while in fact, the segment can escape the perimeter towards the interior thus reducing the energy dissipation.

An alternative estimate of α can be obtained using the general relation [29] $t_m \sim R^2/D_{\mathrm{ch}} = R^2\zeta_{\mathrm{ch}}/(k_BT)$, where ζ_{ch} is the total friction constant of the whole chain. A lower bound on ζ_{ch} is proportional to the number N_{ext} of contacts of a chain with surrounding chains: $N_{\mathrm{ext}} \sim \mathcal{L}/b \propto N^{5/8}$, hence $t_m \propto R^2 N_{\mathrm{ext}} \propto N^{13/8}$ (note that $N_{\mathrm{ext}} \propto N$ in 3D melts leads to the Rouse time [6,29] $t_m \propto N^2$); hence, the lower bound for α is 13/8. Thus, we get $13/8 < \alpha < 15/8$.

The exponent α also defines the shear relaxation modulus $E(t)$ which can be obtained based on the N dependence

of t_m. Applying the standard scaling argument [$E(t)$ must be proportional to the concentration c_0/g of dynamical blobs whose relaxation time $t_m(g) \sim \tau_1 g^\alpha$ is $\sim t$] we get

$$E(t) \simeq k_B T c_0 (\tau_1/t)^{1/\alpha}, \qquad \tau_1 \ll t \ll t_m(N). \quad (1)$$

Our simulation data [21] support this $E(t)$ scaling showing a perfect power law with $\alpha = 1.73 \pm 0.01$ (see Fig. 1). Noteworthy, this α falls in the middle between the theoretical upper (15/8) and lower (13/8) bounds.

Below we focus on the dynamics of a chain c.m. characterized by the mean-square displacement (c.m. MSD) $h(t) = \frac{1}{4}\langle[\underline{r}_{\text{c.m.}}(t) - \underline{r}_{\text{c.m.}}(0)]^2\rangle$ and the c.m. VAF $C(t) = \frac{1}{2}\langle \underline{v}_{\text{c.m.}}(0) \cdot \underline{v}_{\text{c.m.}}(t)\rangle = \ddot{h}(t)$, where $\underline{r}_{\text{c.m.}}$ is the c.m. position vector, $\underline{v}_{\text{c.m.}} = \dot{\underline{r}}_{\text{c.m.}}$, and "dot" means time derivative. The following response-function interpretation of $\dot{h}(t)$ comes from the fluctuation-dissipation theorem [22,30]: Consider the system is at equilibrium at $t = 0$ and a weak external force $\underline{F}/N$ is applied to each unit of a tagged chain at $t > 0$. Then it induces the mean c.m. velocity

$$\langle \underline{v}_{\text{c.m.}} \rangle = \dot{h}(t)\underline{F}/(k_B T). \quad (2)$$

The main physical mechanism for the dynamics is described now. A localized constant force applied to a simple 2D fluid generates a flow $\underline{v}(r, t) = \varkappa(r, t)\underline{F}$, where $\varkappa$ is the half trace of the Oseen tensor

$$\varkappa(r, t) \simeq \frac{1}{4\pi\eta} \ln\frac{\ell(t)}{r}, \qquad r \lesssim \ell(t). \quad (3)$$

The upper cutoff $\ell(t) = \sqrt{\eta t/\rho}$ is the momentum diffusion length (ρ is the fluid density, η is the viscosity) [4,31,32]. According to our key idea [22,23], Eq. (3) is also applicable to polymer systems with slow stress relaxation if η is replaced by the *effective* transient viscosity:

$$\eta \to \eta(t) = \int_0^t E(t)dt. \quad (4)$$

In the intermediate regime $\tau_1 < t < t_m$, we thus get $\eta(t) \sim t^{1-1/\alpha}$, $\ell(t) \sim v_T t^{1-0.5/\alpha}$, $\varkappa(r, t) \sim t^{1/\alpha - 1} \ln[\ell(t)/r]$ if $b \sim \tau_1 \sim 1$ (here $v_T = \sqrt{k_B T/m}$, m is the monomer mass, and we set $k_B T = 1$). Taking into account that the force F in Eq. (2) is actually delocalized within a region of size R, we thus get $\dot{h}(t) \sim \varkappa(R, t) \sim t^{1/\alpha - 1} \ln[\ell(t)/R]$,

$$h(t) \sim t^{1/\alpha} \ln\frac{\ell(t)}{R}, \qquad 1 \ll t \ll t_m; \quad (5)$$

i.e., the c.m. MSD points to an anomalous subdiffusion.

The c.m. MSD predicted in Eq. (5) is totally different from the result in Ref. [9] using an *ad hoc* argument focused on the tagged chain perimeter diffusion: the c.m. MSD $h_{\text{pd}}(t) \sim N^{-1/2} t^{(3/2\alpha)}$, $1 \ll t \ll t_m$. It is clear that the perimeter diffusion ([9]) is always negligible as compared with the collective flow effect. Therefore, our main message: the c.m. dynamics are dominated by the effect of the polymeric VHI.

Quantitative approach.—The above conclusion is fully supported by the quantitative theory outlined below. We focus on the c.m. VAF being more sensitive to reveal the anomalous diffusion [22,23]. Based on Eq. (2) and the generalized equations of slow incompressible 2D fluid dynamics we find (cf. Refs. [22,23,33])

$$C(t) \simeq \frac{k_B T}{N} \int F(q)\kappa(q, t)\frac{d^2 q}{(2\pi)^2}, \qquad t \ll t_m, \quad (6)$$

where $\kappa(q, t) = \frac{d}{dt}\varkappa(q, t)$, $\varkappa(q, t)$ is the Fourier transform of the Oseen function $\varkappa(r, t)$. The Laplace transform of $\kappa(q, t)$ is

$$\hat{\kappa}(q, p) = \frac{1}{2}[\rho p + q^2 \hat{E}(p)]^{-1}, \quad (7)$$

where $\rho = mc_0$ and $\hat{E}(p) = \int E(t)e^{-pt}dt \simeq \Gamma(1 - 1/\alpha)p^{1/\alpha - 1}$ accounts for viscoelastic effects. The form factor $F(q) = N^{-1}\sum_{i,j}\langle\exp[i\underline{q} \cdot (\underline{r}_i - \underline{r}_j)]\rangle$, where i, j are units of a tagged chain. For length scales exceeding the monomer size, $1/q \gg 1$, it shows a universal behavior backed by our simulations: $F(q) \simeq N f(q^2 R^2)$, with $f(x) \simeq 1$ for $x \ll 1$ and $f(x) \sim x^{-11/8}$ for $x \gg 1$ [18]. Using Eq. (6), we get

$$C(t) \simeq v_T^2/(2N), \qquad t \ll t_0, \quad (8)$$

$$C(t) \simeq -C_0 t^{-2+(1/\alpha)}\left[C_1 + \left(2 - \frac{1}{\alpha}\right)\ln\frac{t}{t_0}\right], \quad t_m \gg t \gg t_0, \quad (9)$$

where $C_0 = \sin(\pi/\alpha)(1 - 1/\alpha)/(8\pi^2) \approx 0.0052$, $C_1 \approx 0.259$, $m^* \equiv 0.476 b^2/(v_T \tau_1)^2$, and $t_0 = (N m^*)^{\alpha/(2\alpha-1)}\tau_1$ is the time of momentum diffusion over the whole coil

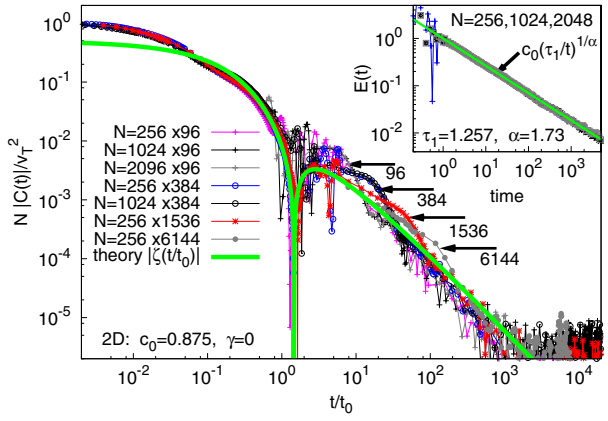

FIG. 1 (color online). The reduced c.m. VAF vs t/t_0. Thick line—theoretical function $\zeta(t/t_0)$ for ∞ box size and $\gamma = 0$. The symbols—simulation data for momentum-conserving dynamics, various chain lengths and system sizes. Around the sign inversion point $\approx 1.45 t_0$, the data are superposed with oscillations due to sound modes [34]. Steps related to the finite box size are marked with arrows: the data of different chain lengths superpose perfectly for the same number of chains. Inset: Shear relaxation function $E(t)$, symbols—simulation data, the line is adjusted according to Eq. (1) to determine $\tau_1 = 1.257$ and $\alpha = 1.73$.

defined by the condition $\ell(t_0) = R$. The c.m. VAF, Eq. (9), is in agreement with the c.m. MSD, Eq. (5).

More generally, we find $C(t) \simeq (v_T^2/N)\zeta(t/t_0)$, where the calculated universal function $\zeta(t/t_0)$ is shown in Fig. 1 together with our momentum-conserving simulation data for various chain lengths and system sizes. The predicted $C(t)$ is negative for $t > t_{\rm inv} \approx 1.45t_0$. A good quantitative agreement can be observed at $t/t_0 \lesssim 10$; however, it deteriorates at longer t as marked by a step feature (a shoulder) shown by arrows. This discrepancy is associated with the finite box size: the simulations are done in a square box $L \times L$, $L = R\sqrt{n_{\rm ch}}$, with periodic boundary conditions. A discrete set of wave vectors is selected in this case: $\underline{q} = (q_1, q_2) = \frac{2\pi}{L}(n_1, n_2)$ with integer n_1, n_2. The c.m. VAF is then defined by Eq. (6), where $\int \frac{d^2q}{(2\pi)^2}$ is replaced by $\frac{1}{L^2}\sum_{\underline{q}\neq 0}$ involving summation over the discrete set of $\underline{q}$ (the condition $\underline{q} \neq 0$ accounts for identically zero total momentum). Using thus modified Eq. (6) we arrive at

$$C(t) \simeq (v_T^2/N)[\zeta(t/t_0) + (1/n_{\rm ch})\zeta_{\rm box}(t/t_L)], \quad (10)$$

where $t_L = t_0[n_{\rm ch}/(2\pi)^2]^{\alpha/(2\alpha-1)}$ is the time of momentum diffusion over the whole box ($\ell(t_L) \sim L$) and the new universal function $\zeta_{\rm box}(t/t_L)$ represents the finite box-size effect. The prediction, Eq. (10), is in agreement with the simulation data in the whole time window of good statistics (see Fig. 2). Note, in particular, how well the steplike

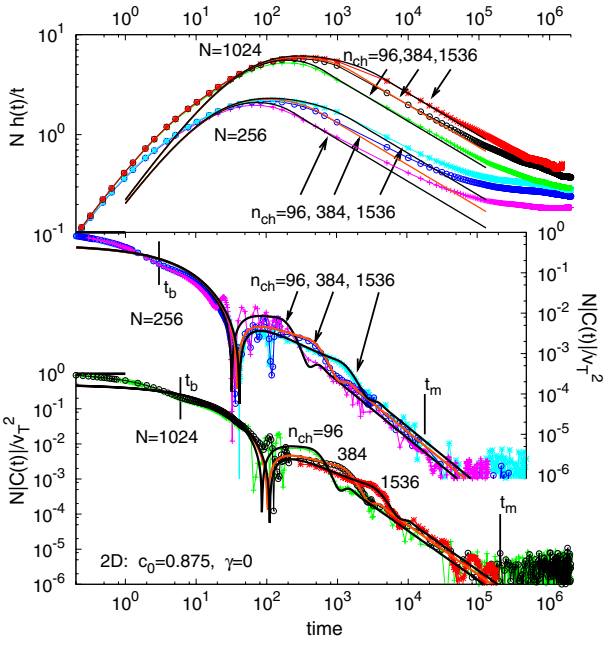

FIG. 2 (color online). c.m. VAF for $N = 1024$ (bottom), $N = 256$ (middle) and c.m. MSD (top); all data are multiplied by chain length. Simulation data is represented by symbols, theory by lines. The MSD for a given chain length split at long times according to the different box size. The theory includes the finite box size term according to Eq. (10) which perfectly describes the step feature of the simulation data [34].

feature at $t \sim 10t_L$ is represented by the theory (this step is also visible in the monomer VAF, not shown).

To resume, we briefly discuss finite compressibility effects. These are twofold. (i) A prolonged ballistic regime, $C(t) \simeq C(0) = \frac{1}{mN}$ for $t \ll t_b$, where the ballistic time t_b *increases* with N, $t_b = R/c_s \propto \sqrt{N}$, where c_s is the sound velocity. Recall that the chains in 2D are *segregated* in regions of size R. The initial momentum P_0 of a tagged chain propagates on the distance $l_s = c_s t$; hence the lion's share of P_0 remains with the chain for $t \ll t_b$. Equation (8) is applicable at longer times, for $t_b \ll t \ll t_0$ (momentum-diffusion regime). The transition between the two short-time regimes is visible as an undulation at $t \sim t_b$ (see Figs. 1–3; note that $t_0/t_b \propto N^{0.2}$). (ii) Reflected sound waves: In a finite box (L) they give rise to oscillations of $C(t)$ with the main period $t_{sL} = L/c_s$ and the longest viscous damping time $t_{\rm damp} \sim L^2\rho/\eta(t_{sL}) \sim \tau_1(c_s/v_T)^2[L/(c_s\tau_1)]^{1+1/\alpha}$ [34].

Langevin dynamics.—We also considered 2D polymer dynamics modified with Langevin friction force $f_L = -\gamma m v$ (v is monomer velocity) applied to each monomer (and the corresponding random noise). Such Langevin dynamics are widely employed in computer simulations. In the confined 2D case the Langevin forces are also directly relevant accounting for the friction between polymer and the supporting surface. Equation (6) is still applicable here, with one change: ρp in the response function, Eq. (7), must be replaced with $\rho(p + \gamma)$ [22,23,33]. The range of the VHI is now defined by the Langevin screening length [35] $\tilde{r} \sim \sqrt{\eta/\rho\gamma}$. It is important that $\tilde{r}$ increases with time in polymer fluids following the effective viscosity $\eta(t)$ [36]: $\tilde{r}(t) \sim (b/\sqrt{m^*\tau_1\gamma})(t/\tau_1)^{(\alpha-1)/(2\alpha)}$ for $t < t_m$. The c.m. VAF can be expressed in terms of the generalized reduced function depending on $\tau = t/t_0$ and $g = \gamma t_0$: $C(t) = (v_T^2/N)\zeta_L(t/t_0, \gamma t_0)$. For $g \gg 1$ it shows the following asymptotic behavior: $\zeta_L(\tau, g) \simeq 0.5e^{-g\tau}$, $\tau \lesssim 1/g$; $\zeta_L \simeq -0.16g^{-11/8}\tau^{z-1}$, $1/\gamma \ll t \ll t_\gamma$; $\zeta_L \simeq -0.0109\tau^{-2+1/\alpha}[1.006 + (1 - 1/\alpha)\ln\tau - \ln g]$, $t_\gamma \ll t \ll t_m$. Here, $z = (3/8)(\alpha - 1)/\alpha$, and $t_\gamma = t_0(\gamma t_0)^{\alpha/(\alpha-1)} = \tau_1(m^*\tau_1\gamma N)^{\alpha/(\alpha-1)}$ is the Langevin characteristic time defined by the condition $\tilde{r}(t) \sim R$; note that $1/\gamma \lesssim t_\gamma \ll t_m$ in the regime $1/t_0 \lesssim \gamma \ll \gamma^*$ we consider [36].

The box-size effects are rather weak for Langevin systems (for $g \gtrsim 1$) and can be neglected in the regime $t \lesssim t_m$, except for short chains $N \lesssim N^* = (m^*\tau_1\gamma n_{ch}/4\pi^2)^{-1/(2-\alpha)}$. Typically $N^* \lesssim 10$, so the latter regime is not important. Thus, the c.m. dynamics are defined by fading inertial effects for short time $t \lesssim 1/\gamma$ [positive decreasing $C(t)$], while the VHI effects control the dynamics at longer times, $t \gg 1/\gamma$. $C(t)$ is negative at $t > t_{\rm inv}$, where $t_{\rm inv}$ is now $\sim 1/\gamma$; more precisely, it is defined asymptotically by $\gamma t \simeq \ln[3.1\gamma t_\gamma (t/t_\gamma)^{0.842}]$. The c.m. VAF behaves as $C(t) \propto -t^{-0.84}$ in the first VHI regime, $t_{\rm inv} \lesssim t \lesssim t_\gamma$, and $C(t) \propto -t^{-1.42}$ in the second VHI regime, $t_\gamma \lesssim t \lesssim t_m$.

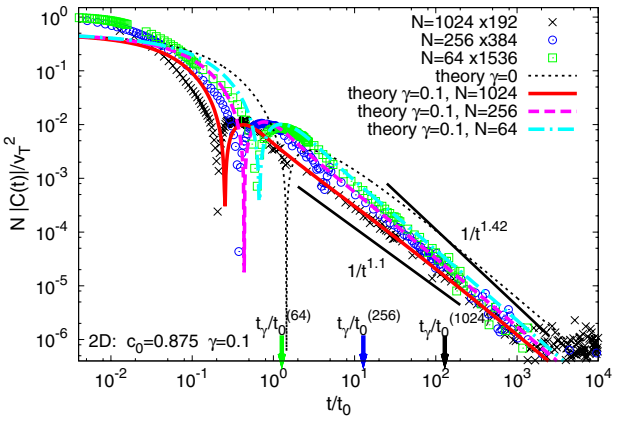

FIG. 3 (color online). c.m. VAF vs t/t_0 with Langevin friction $\gamma = 0.1$. Symbols represent simulation data, lines theory. The thin dashed line shows the infinite-size curve for $\gamma = 0$.

The predictions of the theory [based on the modified Eq. (6)] are compared with the simulation data in Fig. 3 showing a very good agreement (no fitting parameter). The main effects of the friction γ are a significantly shorter sign-inversion time $t_{\rm inv}$, a significantly lower reduced c.m. VAF $N|C(t)|$ for $t \gtrsim t_{\rm inv}$ (it decreases with both γ and N), and a slower decrease of $|C(t)|$ in the intermediate time regime $t_{\rm inv} \lesssim t \lesssim t_\gamma$. The effect of γ on the c.m. dynamics diminishes at longer t (in the second VHI regime). The $t^{-0.84}$ scaling is not visible unless N is very long. In practice both VHI regimes merge giving a broad regime ($t_{\rm inv} \lesssim t \lesssim t_m$) where the slope s of $\ln|C(t)|$ vs $\ln t$ is roughly in the range -1.2 to -1.4; $|s|$ increases with time but decreases with friction γ tending to $|s| \lesssim 1.1$–1.2 for $\gamma \gtrsim 0.5$ (cf. Ref. [9]).

Discussion.—The confined polymer dynamics (the model with Langevin friction in particular) are fundamental and are highly relevant experimentally for polymers adsorbed on solid [10–12,14] or liquid surfaces [7,8] (Langmuir polymer films), or trapped on surfactant membranes (supported phospholipid bilayers) [6,11,13]. The dynamics are relevant to important technological and biomimetic applications [11,37]. Understanding of the 2D polymer diffusion can also shed light on the dynamics of protein motions in cell membranes [27,38]. Curiously, the predicted anomalous subdiffusive MSD $h(t) \propto t^{1/\alpha} \approx t^{0.58}$ is rather close to the subdiffusion anomaly of transmembrane proteins ($t^{0.65\pm0.05}$) [27], although the membrane system cannot be regarded as closely a 2D melt. The chain conformational relaxation time, $t_m \propto N^\alpha$ with $\alpha \approx 1.73$ coming from our model (without chain crossings) is in harmony with recent results for polymers confined at air-water interface [8] [see Fig. 3b there]. Noteworthy, for $\gamma > \gamma^*(N)$ we predict Rouse-like $t_m \propto N^2$, $D \propto 1/N$ which is consistent with recent measurements on polymer surface diffusion [10,39]. However, in some cases the hydrodynamic coupling to the third dimension may need to be considered as well [25,26] which deserves further investigation.

Conclusion.—We elucidated the physical origin of the highly correlated chain dynamics in 2D melts: We demonstrated, both analytically and numerically, that the VHI effects are extremely important. Our quantitative analytical theory of anomalous subdiffusion in polymer monolayers predicts a complex behavior of the c.m. VAF controlled by a delicate interplay of inertial, viscoelastic, finite-box-size, and frictional effects. The theoretical c.m. VAF and MSD are in remarkably good quantitative agreement with our simulation data without fitting parameters. By contrast, the fractal chain perimeter friction effects [9] are shown to be subdominant; hence, the theory of Ref. [9] has probably no region of applicability. The obtained c.m. VAF in the intermediate regime (t shorter than the polymer relaxation time t_m) is different in both the sign and decay law from the classical $t^{-d/2} = t^{-1}$ power decay found in simple 2D fluids. Eq. (9) is even not a pure power law. We also discovered the basic scaling laws for the chain relaxation time, $t_m(N) \propto N^\alpha$, and the relaxation modulus, $E(t) \propto t^{-1/\alpha}$, with $\alpha = 1.73 \pm 0.01$ pointing to a new dynamical exponent for 2D melts. In addition, the time growth of the Langevin screening length $\tilde{r}(t)$ explains why both the dominance of the VHI effects and the highly cooperative polymer motions are preserved even with the Langevin friction.

We acknowledge partial support by the French ANR Grant 'DYNABLOCKs' (ANR-09-BLAN-0034-01), computer resources by PMNA/ENIAC, and discussions with A. Johner, J. Farago, J. Wittmer, and J. Baschnagel.

[1] B. J. Alder and T. E. Wainwright, Phys. Rev. A **1**, 18 (1970).
[2] K. Kawasaki, Phys. Lett. A **32**, 379 (1970); Prog. Theor. Phys. **45**, 1691 (1971).
[3] Y. Pomeau and P. Résibois, Phys. Rep. **19**, 63 (1975).
[4] T. Petrosky, Found. Phys. **29**, 1417 (1999); **29**, 1581 (1999).
[5] M. Isobe, Phys. Rev. E **77**, 021201 (2008).
[6] P. G. de Gennes, *Scaling Concepts in Polymer Physics* (Cornell University Press, Ithaca, New York, 1979).
[7] N. Sato, S. Ito, and M. Yamamoto, Macromolecules **31**, 2673 (1998).
[8] S. Srivastava and J. K. Basu, J. Chem. Phys. **130**, 224907 (2009).
[9] J. P. Wittmer, H. Meyer, A. Johner, T. Kreer, and J. Baschnagel, Phys. Rev. Lett. **105**, 037802 (2010).
[10] J. Wong, L. Hong, S. Bae, and S. Granick, Macromolecules **44**, 3073 (2011).
[11] S. C. Bae and S. Granick, Annu. Rev. Phys. Chem. **58**, 353 (2007).
[12] S. Sukhishvili, Y. Chen, J. D. Müller, E. Gratton, K. S. Schweizer, and S. Granick, Nature (London) **406**, 146 (2000).
[13] B. Maier and J. O. Rädler, Phys. Rev. Lett. **82**, 1911 (1999).
[14] J. Zhao and S. Granick, Macromolecules **40**, 1243 (2007).

[15] B. Duplantier, J. Stat. Phys. **54**, 581 (1989).
[16] A. Semenov and A. Johner, Eur. Phys. J. E **12**, 469 (2003).
[17] A. Cavallo, M. Müller, and K. Binder, J. Phys. Chem. B **109**, 6544 (2005).
[18] H. Meyer, T. Kreer, M. Aichele, A. Cavallo, A. Johner, J. Baschnagel, and J. Wittmer, Phys. Rev. E **79**, 050802 (2009); J. Chem. Phys. **132**, 184904 (2010).
[19] I. Carmesin and K. Kremer, J. Phys. (Paris) **51**, 915 (1990).
[20] Here we consider such 2D systems (polymer monolayers) where chains are not entangled due to high energetic penalty for chain crossings [6–9,13,15–17].
[21] All simulation data reported in this Letter are obtained with the same generic bead-spring model as used in the previous work on 2D systems [9,18] at high-melt density $c_0 = 0.875$. All results are reported in Lennard-Jones units. In contrast to Refs. [9,18], here we mainly report dynamic data of momentum-conserving simulations and weaker Langevin friction using the same algorithms as for our work on 3D melts [22].
[22] J. Farago, H. Meyer, and A. N. Semenov, Phys. Rev. Lett. **107**, 178301 (2011).
[23] J. Farago, H. Meyer, J. Baschnagel, and A. N. Semenov, Phys. Rev. E **85**, 051807 (2012).
[24] O. Punkkinen, E. Falck, I. Vattulainen, and T. Ala-Nissila, J. Chem. Phys. **122**, 094904 (2005).
[25] T. G. Desai, P. Keblinski, and S. K. Kumar, J. Chem. Phys. **128**, 044903 (2008).
[26] S. Ramachandran, S. Komura, K. Seki, and G. Gompper, Eur. Phys. J. E **34**, 46 (2011).
[27] U. Schmidt and M. Weiss, J. Chem. Phys. **134**, 165101 (2011).
[28] Hu-Jun Qian, Li-Jun Chen, Zhong-Yuan Lu, and Ze-Sheng Li, Phys. Rev. Lett. **99**, 068301 (2007).
[29] M. Rubinstein and R. H. Colby, *Polymer Physics* (Oxford University Press, Oxford, UK, 2003).
[30] L. D. Landau and E. M. Lifshitz, *Statistical Physics* (Pergamon, Oxford, 1998).
[31] J. P. Hansen and I. R. McDonalds, *Theory of Simple Liquids* (Academic Press, New York, 2006).
[32] M. Doi and S. F. Edwards, *The Theory of Polymer Dynamics* (Oxford University Press, Oxford, 1996).
[33] A. N. Semenov, J. Farago, and H. Meyer, J. Chem. Phys. **136**, 244905 (2012).
[34] The fading oscillations due to sound waves have been smoothed out for $t > 200$ to make the step better visible.
[35] P. Ahlrichs, R. Everaers, and B. Dünweg, Phys. Rev. E **64**, 040501 (2001); B. Dünweg, J. Chem. Phys. **99**, 6977 (1993); P. Ahlrichs and B. Dünweg, J. Chem. Phys. **111**, 8225 (1999).
[36] The relaxation modulus $E(t)$ is not affected by γ if $\gamma \ll \gamma^* = 20\upsilon_T^2\tau_1 c_0 N^{\alpha-2}$ ($\gamma^* \gtrsim 3.4$ for the chain lengths considered).
[37] D. Ho, B. Chu, J. J. Schmidt, E. K. Brooks, and C. D. Montemagno, IEEE Trans. Nanotechnol. **3**, 256 (2004).
[38] K. Ritchie, X.-Y. Shan, J. Kondo, K. Iwasawa, T. Fujiwara, and A. Kusumi, Biophys. J. **88**, 2266 (2005).
[39] While the reptationlike $N^{-1.5}$ scaling of single-chain diffusion constant was measured in two dimensions [11,12], it was later revealed that it is mainly due to surface inhomogeneities rather than to topological effects [10,28] which are suppressed anyway in 2D monolayers where chains do not intersect [6–9,13].